CHAPTER 4

A Facile Synthesis of Green-Blue Carbon Dots from *Artocarpous lakoocha* Seeds and Their Application for the Detection of Iron (III) in Biological Floods and Cellular Imaging

4.1 Introduction

Carbon dots (CDs) first prepared by Xu. et al., in 2004 through electrophoresis, are novel fluorescent carbon nanoparticles having a diameter below 10 nm and are mainly consists of carbon, hydrogen, and oxygen [Xu *et.al*. (2004), Xu *et.al*. (2015)]. CDs have fascinated enormous attention around the world due to their dazzling properties like higher fluorescence intensity [Liang *et.al*. (2013)], good solubility [Yan *et.al*. (20185], easy surface functionalization, [Ting *et.al*. (2015)], low toxicity, and good biocompatibility [Yang *et.al*. (2009)]. The outstanding properties of CDs provide excellent material for the scientific community due to its potential application in a different area of chemistry and biology including bioimaging [Antaris *et.al*. (2013)], biosensors [Zhu *et.al*. (2013)], drug delivery systems [Feng *et.al*. (2016)], catalysis and optronics [Hu *et.al*. (2013), Ma *et.al*. (2015)]. During the last decade, varieties of method have been developed by many of the research group for the preparation of carbon dots such as ultrasonic [Li *et.al*. (2011)], thermal decomposition, electrochemical synthesis [Li *et.al*. (2010)], microwave [Li *et.al*. (2016)], hydrothermal synthesis [Du *et.al*. (2016)] and combustion oxidation [Rahy *et.al*. (2012)]. Amid them, a hydrothermal method is superior due to its various advantages including single step, no requirement of post-treatment, low energy consumption, simple operating conditions, low-cost apparatus, etc [Wang *et.al*. (2017), Prasannan *et.al*. (2013)].

In biological systems, iron (Fe) is considered to be the most important transition metal as well as is the fourth richest element in the earth crust. Iron is a vital ingredient of hemoglobin which facilitates the transport service of blood in the human body [Crichton *et.al*. (2008)]. The insufficiency of iron causes many health problems in the human being like anemia, loss of

appetite, frequent fatigue, reduced work routine and decreased immunity. Whereas overload accumulation of iron in blood encourages a variety of biological disorders such as fibrosis, tissue damage of different organs and production of reactive oxygen species which results in deterioration of proteins, nucleic acids and lipids [Troeppner *et.al.* (2014), Bruijnincx *et.al.* (2008)]. Hence, for better human health, observation of concentrations of iron in biological fluids is imperative [Ju *et.al.* (2014)]. Recently, varieties of technique such as spectrophotometry [Garcia-Marco *et.al.* (2006)], atomic absorption/emission spectrometry [Li *et.al.* (2013)], electrochemical methods [Kindra *et.al.* (2015)] etc., have been applied to determine Fe^{3+} concentration. However, these methods are expensive, a requirement of specific instrumentations, trained operator and time-consuming. These limitations prevent their practical applications [Buduru *et.al.* (2016)]. Contrary to this, due to high sensitivity, simplicity, fast response time and excellent resolution, the fluorescent-based assay has attracted great attention towards rapid and sensitive detection of Fe^{3+} ion. Although, several materials including metal-organic framework (MOFs), gold nanoclusters, reduced graphene oxide (r-GO), organic fluorescent dyes have been reported as a fluorescent sensor for the recognition of Fe^{3+} ion, still they have some drawback. For instance, due to complication in the synthesis and purification steps, metal-based nanomaterials are incapable of simple and fast detection while due to poor water solubility, toxicity and rapid photobleaching, organic fluorescent dye-based probes are also not suitable for sensing of Fe^{3+} ion in the living cells. Although several investigations have been carried out on sensing of Fe^{+3} using carbon dots (CDs) but the precursors used to synthesize these CDs were mostly chemically derived, i.e., from passivation of expensive and toxic heteroatom's. However, the use of non eco-friendly materials with multistep preparation made it tedious procedure resulting in limitations of their applications [Salam *et.al.* (2012)]. On the other

hand, the natural pioneers are excellent alternate over harmful chemicals for the preparation of CDs due to numerous benefits including low price, nontoxicity, good biocompatibility and high abundance [Zhang *et.al*. (2018), Yadav *et.al*. (2019), Lie *et.al*. (2012)]. Therefore, the expansion of simple and green precursor based CDs is imperative to keep away from such limitations.

To address these limitations herein, we have prepared CDs from the seeds of Artocarpus *lakoocha* for the first time (**Scheme4.1)**.

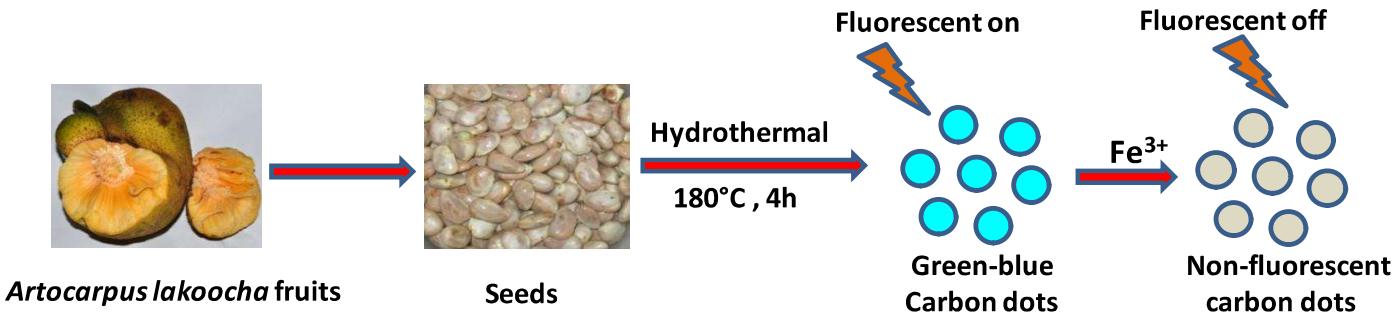

Scheme 4.1 Schematic diagram for the synthesis of GB-CDs and their application in Fe^{3+} detection.

Interestingly, the as-synthesized CDs displayed green-blue emission under Ultra-Violet (UV) light hence named it green-blue carbon dots (GB-CDs). As-synthesized GB-CDs were fully characterized through a variety of instrumental techniques such as UV-visible, fluorescence spectroscopy, TEM, XRD, XPS, zeta potential and FT-IR spectroscopy. Further, the fluorescence stability tests of GB-CDs were performed in various parameters such as pH, the higher concentration of NaCl and continuous irradiation in visible light approximately three

months. These CDs were capable of detecting Fe^{3+} ion selectively with a good quantum yield. In addition, GB-CDs were employed to detect Fe^{3+} in river water as well as in human blood serum, which showed practical potential for different bio-applications. Finally, MTT assay was performed on SH-SY5Y neuroblastoma cells and results showed negligible cytotoxicity, revealing that GB-CDs could be potentially used in intracellular imaging as a fluorescent probe.

4.2. Experimental section

4.2.1. Materials

The fresh fruits of *Artocarpus lakoocha* were obtained from the campus of IIT (BHU), Varanasi, U.P., India. From the fruits, the seeds were collected and washed thoroughly with distilled water to remove the dust particles. All tentative materials were procured from commercial suppliers. The entire experiments were carried out in distilled water. The metals used for sensing purpose were purchased from Sigma Aldrich, India. $FeCl_3$ salt was used to prepare Fe^{3+} solution, while nitrate salts were used to prepare other metal solutions. The stock solution of Fe^{3+} (10^{-2} M concentration) was prepared by adding 16 mg $FeCl_3$ in 10 ml distilled water. Further by diluting the stock solution, the other concentrations were obtained (10^{-3} to 10^{-6}M).

4.2.2. Hydrothermal Synthesis of green-blue carbon dots

Initially, 5g *Artocarpus lakoocha* seeds were crushed into small pieces and dissolved in 150 mL of distilled water. Afterward, the suspension was poured in 250 mL Teflon-line stainless steel autoclave and kept in a hot air oven at 180 °C for 4 hours. When the reaction completed, the autoclave was cooled and the find solution was centrifuged at 14000 rpm for 15 min to eliminate the agglomerated and larger particles. After then, the solution was dialyzed for 24 h in distilled water and finally obtained pure light-brown color CDs and stored for further utilize.

4.2.3. Apparatus and characterization

Transmission electron microscopy (TEM) images were acquired on a (TEM, TECHNAI 20 G2) at the accelerating voltage 200 kV. Energy dispersive X-ray spectroscopy (EDAX) was acquired through the TEM analysis. By using Nano Zeta Sizer Malvern apparatus (4.0 mW laser), zeta potential was carried out. The Powder X-ray diffraction (P-XRD) were acquired on a Rigaku Smart lab between 2θ = 5-80°. The Fourier transform infra-red (FTIR) spectrum of GB-CDs was performed on KBr pellets with Perkin Elmer Spectrum 100 from 4000 to 500 cm^{-1}. X-ray photoelectron spectra (XPS) were recorded on (AMICUS, kratuos, Analytical, Ashimadzu) with Mg Kα excitation (1253.6 eV) radiation. UV-vis spectra were performed on Thermo scientific EVOLUTION 201 spectrophotometer at 200-800 nm. The emission experiments and the fluorescence lifetimes were measured on Edinburgh instrument FLS 980 fluorescence spectrophotometer.

4.2.4. Quantum yield measurements

The QY of as-prepared GB-CDs was calculated comparative to that of quinine sulfate (QY = 54 % at 360 nm excitation). The optical density (below 0.1) and the integrated intensity of the quinine sulfate solution in 0.1 M H_2SO_4 were also measured. For GB-CDs, the equivalent measurements were performed with similar parameters and QYs were determined through **Table 4.1.**

4.2.5. Detection of Fe^{3+} ion in real samples

The detections of Fe^{3+} ion were performed in river water as well as in human blood serum. Firstly the river water was collected from the Ganga River (Varanasi, India). To remove large and agglomerated particles, the water samples were filtered through 0.22 μm membrane

(Millipore). After then, in 80 µL of GB-CDs solution (6 mg mL^{-1}), 15 µL of river water and 15 µL of different concentrations of Fe^{3+} solution (20, 40, 60 and 80 µM) were mixed and fluorescence emission spectra were carried out. Further, recovery efficiency was calculated by using the sensing procedure. To sense Fe^{3+} in human blood serum, first of all the serum was treated to release the proteins as precipitate by centrifugation and collected the supernatant for further used. In 1 ml of fluorescent GB-CDs, different volume of deproteinized human serum (25, 50, 75, 100, 125 and 150 µL) was added and fluorescent emission spectra were recorded.

4.2.6. Cytotoxicity assay

To determine the cytotoxicity of as-synthesized GB-CDs, 3-(4,5-dimethylthiazol-2-yl)-2,5-diphenyltetrazolium bromide (MTT) assay was performed on SH-SY5Y neuroblastoma cells. SH-SY5Y neuroblastoma cells were incubated in Dulbecco Modified Eagles Medium (DMEM) and seeded into 96-well cell culture plates at a density of 5×10^4 cells per well at 37 °C for 24 hours. After that, these cells were cultured with different concentrations of GB-CDs (0.01 µg mL^{-1}, 0.1 µg mL^{-1}, 1 µg mL^{-1}, 10 µg mL^{-1}, 100 µg mL^{-1} and 200 µg mL^{-1}) for another 24 hours. After incubation period, the cell viability was determined using MTT assay. Briefly, the medium was replaced with 80 µL of fresh medium and 20 µL of MTT (0.5 mg mL^{-1}, final concentration; Sigma) in phosphate buffer saline (PBS). After 4 h, MTT was removed and the crystals of formazan were dissolved in DMSO. Formazan concentrations were quantified at 570 nm with 630 nm reference wavelengths using Synergy HTX Multi-Mode reader (BioTek, USA). The following **equation 4.1** was utilized to determine cell viability.

$$\text{Cell viability (\%)} = \frac{\text{Absorbance}_{\text{treated}}}{\text{Absorbance}_{\text{control}}} \times 100\% \qquad \textbf{4.1}$$

4.2.7. In vitro imaging study

SH-SY5Y neuroblastoma cells were grown in coverglass bottom dishes cell culture plate in DMEM supplied with 10% FBS followed by culturing the cell in 5% CO_2 at 37°C for 24 hours. The cells then were treated with 200 µg mL^{-1} GB-CDs solution for 15h. After then, in treated cells, 100 µL of $FeCl_3$ solution (10^{-4}) was added and further incubated for 2h. The fluorescent images were recorded under a fluorescence microscope at excitation of 485 nm and 460 nm.

4.3. Results and Discussion

4.3.1. Characterizations

The morphology and size of GB-CDs were investigated through TEM analysis. The results confirmed the spherical morphology **(Figure 4.1A**) and the corresponding histogram represented that the particles are dispersed in the range of 1.5 to 6.5 nm with an average size of 4 nm **(Figure 4.1B).** The selected area electron diffraction (SAED) patterns examined crystal defect and revealed the amorphous nature of GB-CDs **(inset Figure 4.1A).** The XRD study revealed a broad peak at 2θ = 23.5°, which further supported the amorphous nature of GB-CDs **(Figure 4.1C).** [Liang *et.al*. (2019), Li *et.al*. (2018)]. The existence of different functional groups on GB-CDs surface were investigated using FT-IR spectra. The peak at 3426 cm^{-1} attributed to O-H stretching, 2959 and 2848 cm^{-1} associated with C-H stretching and the peak at 1628 cm^{-1} revealed the occurrence of C=O stretching. The peaks at 1457 and 1352 cm^{-1} were associated with C=C and C-N stretching vibration **(Figure 4.1D).** These results showed the presence of

various functional groups like (-OH, -NH_2, and -C=O) [Molkenova *et.al*. (2019), Lin *et.al*. (2015). Rahimi *et.al*. (2019)].

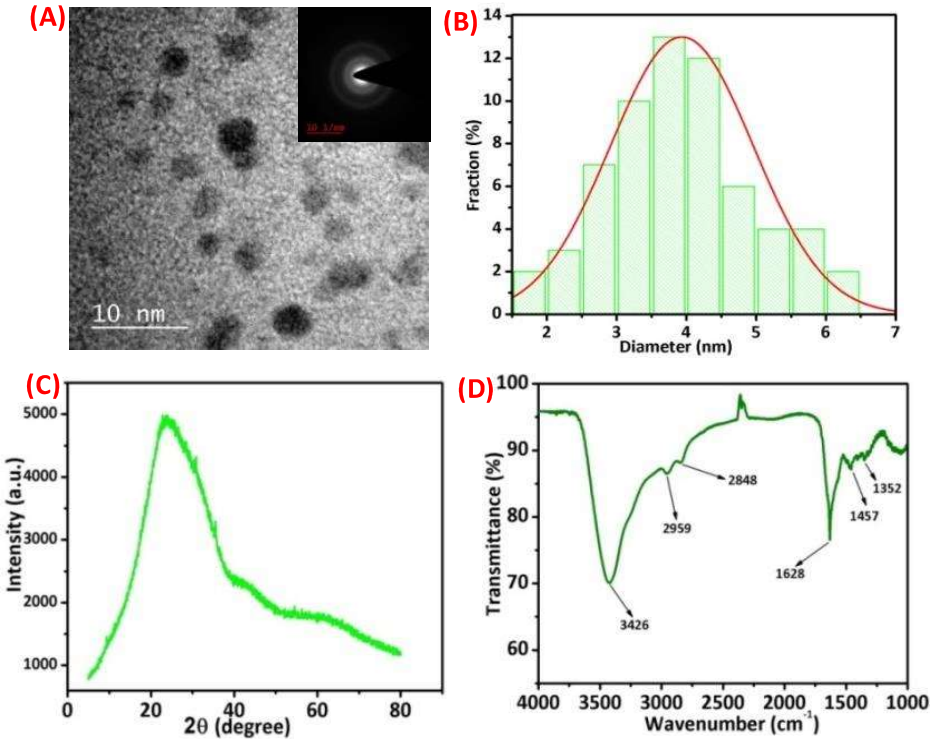

Figure 4.1 (A) HRTEM images of as-prepared GB-CDs, (B) Size distribution histogram, (C) XRD pattern of the GB-CDs and (D) FT-IR spectra of GB-CDs.

Addition to this, the zeta potential of the GB-CDs was -20.26 mV (**Figure 4.2**). The occurrence of the different functional groups not only revealed the negative charge on GB-CDs surface but also advances their stability, electronic properties and hydrophilic character in aqueous systems.

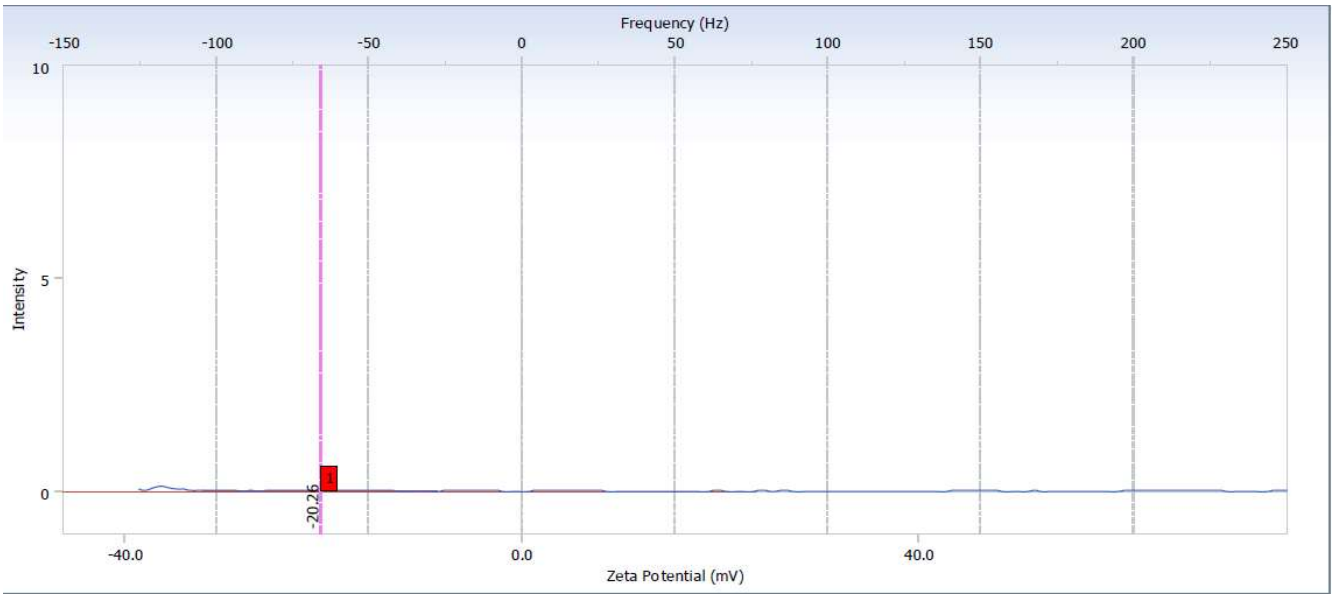

Figure 4.2 Zeta potential of as-synthesized GB-CDs.

To investigate the chemical composition, surface state and the elements present in GB-CDs, X-ray photoelectron spectroscopy (XPS) was carried out**.** The wide scan survey spectrum illustrates the characteristic peaks correspond to C1s (286.49 eV), N1s (400.45 eV) and O1s (534.32 eV), confirmed that GB-CDs were mainly composed of C, N, and O (**figure 4.3A**). The high-resolution C 1s spectrum revealed four peaks located at 285.69, 286.77, 288.64 and 287.64 eV, which ascribed C=C/C-C, C-N, C=O and C-O moieties respectively (**Figure 4.3B**) [Zhuang *et.al*. (2019), Zuo *et.al*. (2019)]. Furthermore, the XPS spectrum of N 1s revealed four peaks at

399.05, 403.10, 401.40 and 400.05 eV ascribed to pyridinic N (Py-N), pyridinic N-O, quaternary N (Q-N) and pyrrolic N (Pr-N) respectively (**Figure 4.3C**) [Xing *et.al*. (2018)]. Moreover, the high-resolution O 1s spectrum exhibited four peaks at 532.98, 535.15, 533.75 and 534.43 eV which corresponded to (C=O), (N=O), (C-O) and (C-OH) respectively (**Figure 4.3D**) [Das *et.al*. (2016), Singh *et.al*. (2018)].

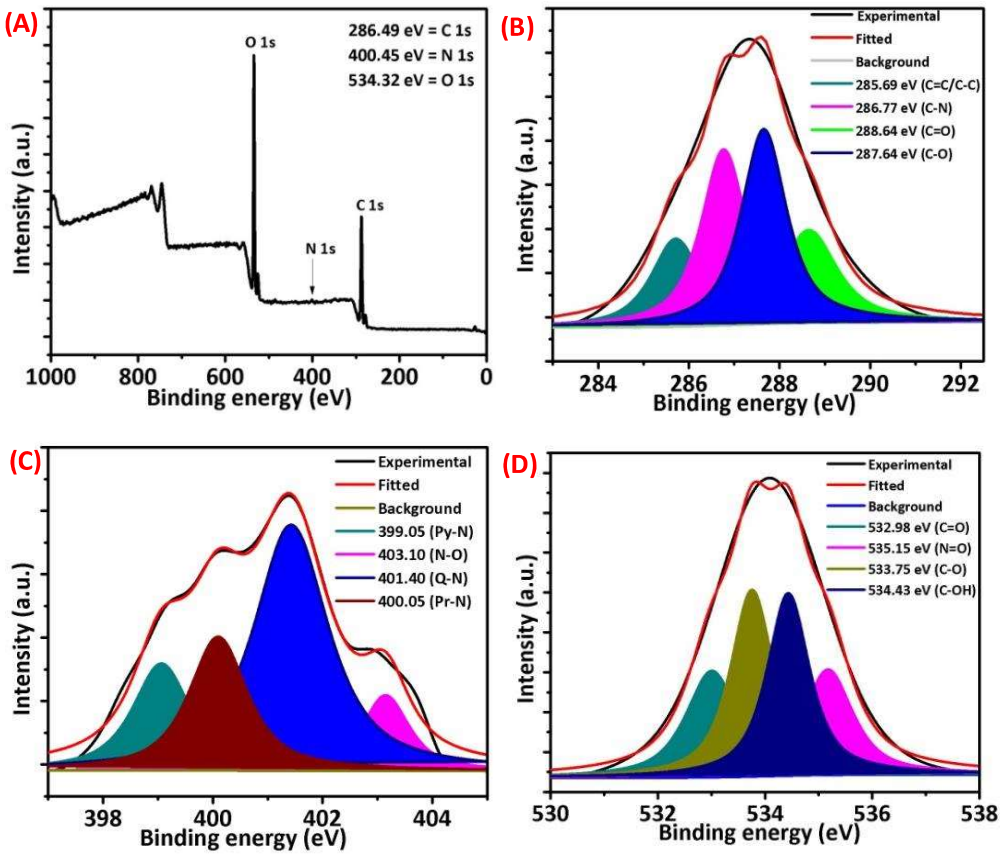

Figure 4.3 (A) XPS survey scan, (B) XPS spectrum of C 1s, (C) XPS spectrum of N 1s and (D) XPS spectrum of O 1s of as-synthesized GB-CDs.

Further, the Energy Dispersive Spectroscopy (EDS) spectrum of GB-CDs revealed the presence of C (58.64%), N (15.83%) and O (25.53%) (**Figure 4.4**). All these experimental analyses revealed the successful synthesis of GB-CDs.

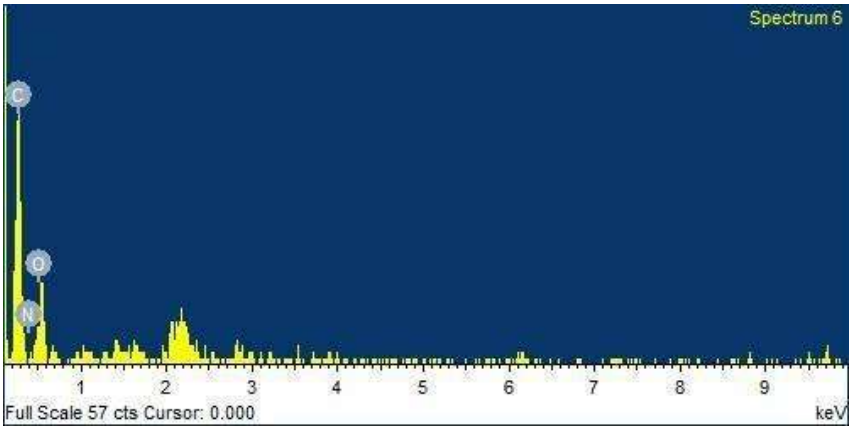

Element	Weight%	Atomic%
C K	52.77	58.64
N K	16.62	15.83
O K	30.61	25.53
Totals	100.00	

Figure 4.4 EDS spectrum of as-synthesized GB-CDs.

4.3.2. Optical properties

The UV-vis absorption spectrum of GB-CDs showed two peaks at 276 nm and 334 nm, which were due to π-π^* of carbon-carbon double bond and n-π^* of the carbonyl compound **(Figure 4.5A)** [Jeong *et.al*. (2018)]**.** The as-prepared GB-CDs exhibited excitation dependent fluorescent

emission spectra on changing the excitation wavelength from 320 nm to 410 nm. Initially, emission intensity increases as the excitation increases from 320 to 350 nm, achieving maximum fluorescence emission intensity (475 nm) at the excitation wavelength of 350 nm, after then a gradual decrease in the fluorescent emission intensity was observed by altering the excitation wavelength from 360 to 410 nm (**figure 4.5B).**

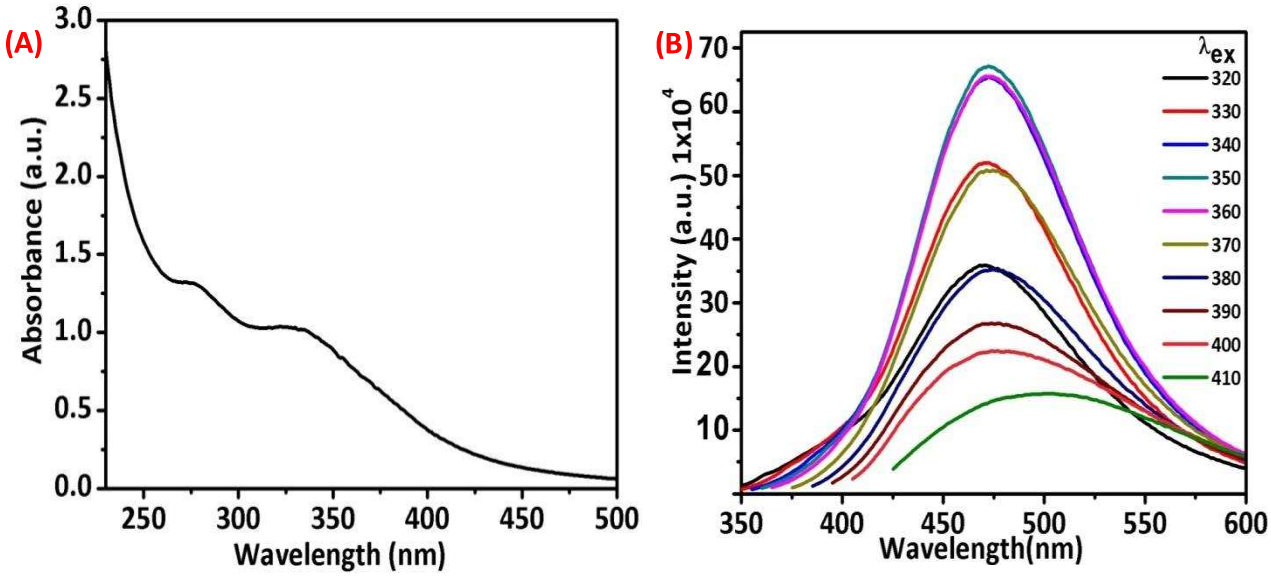

Figure 4.5 (A) UV-vis absorption spectra of GB-CDs (B) Fluorescence emission spectra of GB-CDs at different excitation wavelength (320-410 nm).

The quantum yield of fluorescent GB-CDs was calculated to be 38.5 % taking quinine sulfate (54%) as standard (**Table 4.1**).

Table 4.1 Calculation of fluorescence quantum yield with integrated intensity and absorbance of quinine sulfate and GB-CDs at excitation wavelength 360 nm.

Sample	Integrated intensity at 360 nm	Absorbance at 360 nm	Quantum yield (%)
Quinine sulphate (reference)	55788396	0.053	54
GB-CDs	42808909	0.057	38.5

The fluorescent stability of as-prepared GB-CDs was examined in different parameters such as pH and different concentrations of NaCl salts. It was observed that by changing the pH from 2 to 12, the fluorescent intensity increases up to pH 7, after then gradually decreases from pH 7 to 12 showing that the as-prepared GB-CDs are stable in a wide pH range **(Figure 4.6).**

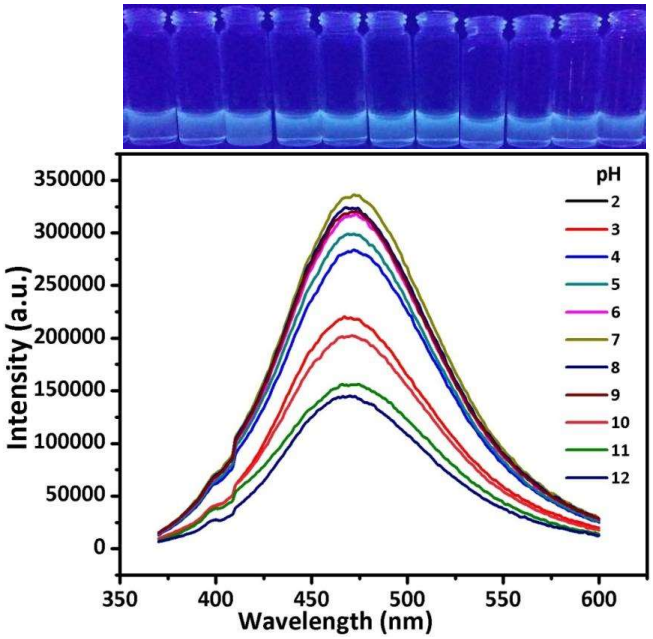

Figure 4.6 Study of pH change on the fluorescent intensity of GB-CDs with corresponding photograph under UV – light (λex = 365 nm) from pH range 2 to 12.

The effect of ionic strength on the fluorescent intensity of GB-CDs was also checked by treating with NaCl solution of different concentrations (0.5 to 5 M) and was observed no significant changes in the fluorescent intensity revealing the non-ionizability and soaring stability of functional groups present on the surface of GB-CDs in higher salt conditions (**Figure4.7).**

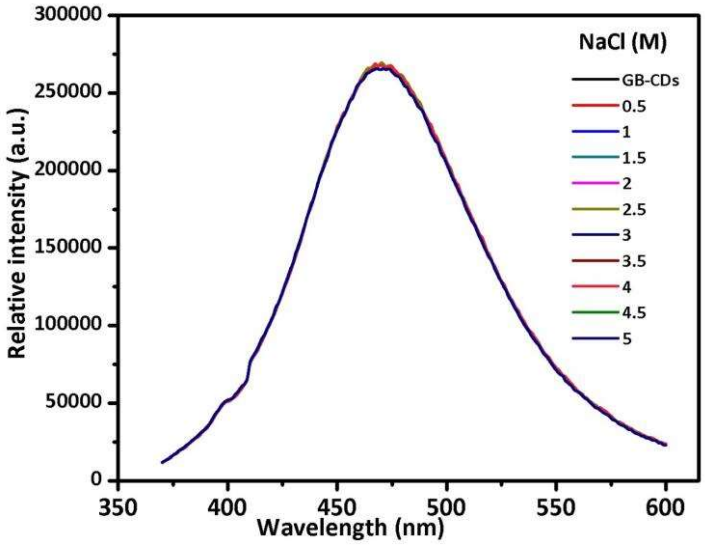

Figure 4.7 Effect of ionic strength on the fluorescent intensity of GB-CDs.

The high photostability was confirmed by treating GB-CDs with visible light about 95 days continuously, which had almost no influence on the fluorescent intensity (**Figure 4.8**). In addition, there were no precipitations obtained to stock up the GB-CDs solution for five months at room temperature, enlightening their long term stability.

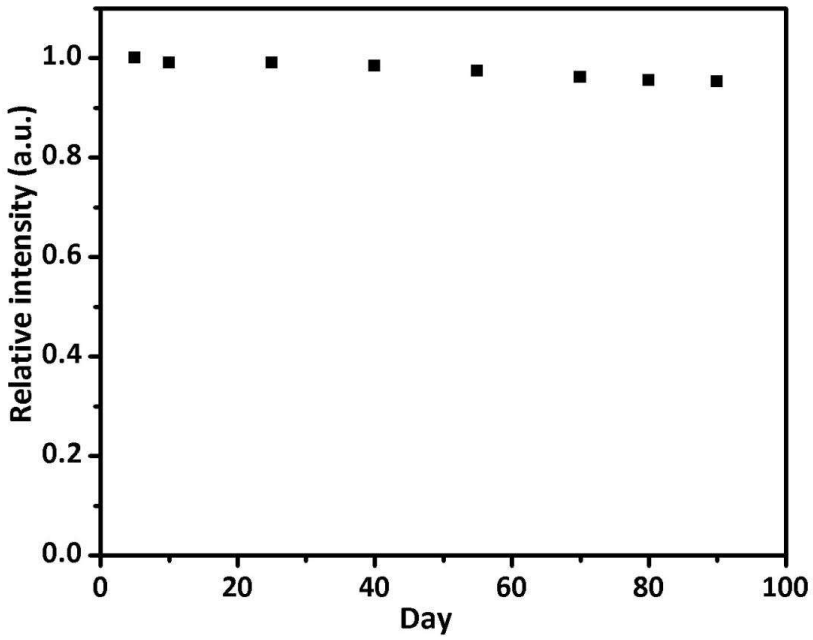

Figure 4.8 Photo stability of as-synthesized GB-CDs under visible-light.

4.4. Selectivity studies

The critical parameters for sensing activities are selectivity and sensitivity. It can be seen from **Figure 4.9** that, in the presence of 15 metal ions (Na^+, K^+, Al^{3+}, Pb^{2+}, Cd^{2+}, Hg^{2+}, Fe^{2+}, Cr^{3+}, Mn^{2+}, Ni^{2+}, Co^{2+}, As^{3+}, Cu^+, Ag^+ and Zn^{2+}), there was almost no effect on the fluorescent intensity of GB-CDs but when a definite concentration of Fe^{3+} was added in the solution, then a remarkable decrease in the fluorescence intensity takes place, revealing the high selectivity of GB-CDs towards Fe^{3+} ion.

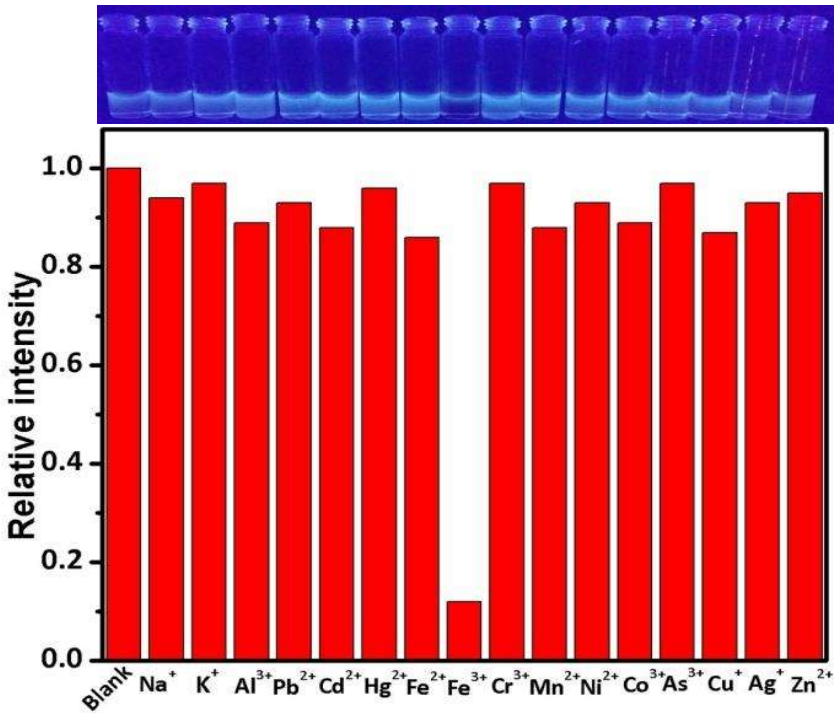

Figure 4.9 Photograph showing the selective sensing of Fe^{3+} ion and bar diagram symbolizes the relative fluorescent intensity of GB-CDs by adding 40 µL of Fe^{3+} solution (10^{-3}M) and 40 µL of other metal ions (10^{-2}M), showing the insignificant interference of other metal ions.

To determine the sensitivity of GB-CDs fluorescent probe towards Fe^{3+} ion, a fluorescent titration experiment was performed by exciting the as-synthesized GB-CDs at its maximum excitation wavelength (350 nm). The maxima fluorescent emission intensity (475 nm) decreased upon the gradual addition of different concentrations of Fe^{3+} solution (0-100 µM) (**Figure 4.10A).**

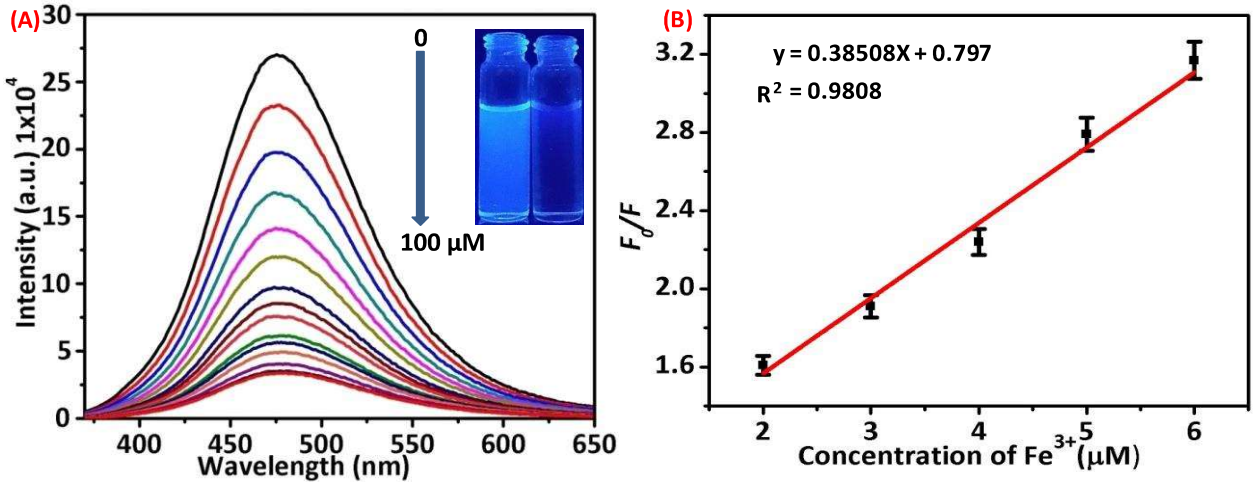

Figure 4.10 (A) Fluorescence titration experiment revealing the quenching upon consecutive addition of Fe^{3+} ion into GB-CDs solution, (B) shows fluorescent detection of Fe^{3+} ion being fitted into Stern-Volmer plot.

The possible fluorescence quenching mechanism is due to the interaction between the quencher molecule (Fe^{3+} ion) and fluorescent molecule (GB-CDs) which probably maybe because of the inner filter effect (IFE), dynamic quenching or static quenching. It can be seen from **Figure 4.11A** that there were two absorption bands at 298 and 450 nm (black line) in the spectrum of Fe^{3+} ion. The GB-CDs exhibited maximum excitation peak at 350 nm (green line) and maximum emission peak at 475 nm (red line). As a result, a fine and precise spectral overlap obtained between the absorption spectrum of Fe^{3+} ion and emission spectrum of as-synthesized GB-CDs. Due to this IFE, Fe^{3+} absorbs the emission light of the fluorophore GB-CDs resulting in the quenching of fluorescence [Huang *et.al*. (2015)].

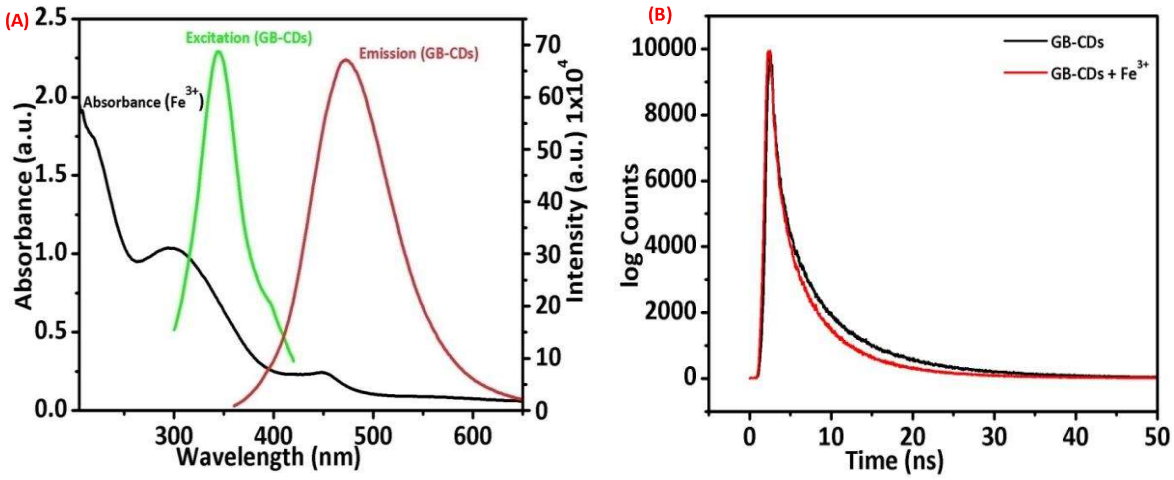

Fig. 4.11 (A) UV- vis absorption spectra of Fe^{3+} (black line), excitation spectra of GB-CDs at λ_{em} = 475 nm (green-line), emission spectra of GB-CDs at λ_{ex} = 350 nm (red line), (B) Fluorescence lifetime decay curve of GB-CDs in the presence and absence of Fe^{3+} ion.

The other most useful technique to differentiate amid IFE, static and dynamic quenching is the fluorescence lifetime study. To gain detail about the quenching mechanism, the fluorescence lifetime investigation of as-synthesized GB-CDs with and without Fe^{3+} was carried out. It can be seen from **Figure 4.11B** and **Table 4.2** that the fluorescence decay profiles were well fitted by a triexponential function with an obvious shift in average lifetimes, i.e. from 7.94 ns to 5.69 ns before and after addition of Fe^{3+}, revealing the excited state interaction between Fe^{3+} and GB-CDs i.e. happening of dynamic quenching. These results strongly confirmed that the fluorescence quenching of as-synthesized GB-CDs was due to a combination of IFE and dynamic quenching [Zu *et.al*. (2017), Feng *et.al*. (2016)].

Table 4.2 Details of fluorescence lifetime measurement of GB-CDs in the presence and absence of Fe^{3+} ion.

Compound	Average life time (ns)	Chi square	Different life time (ns)	Corresponding Weight (%)
GB-CDs	7.94	1.157	τ_1 = 0.64 (B_1=3292.29) τ_2 = 3.25 (B_2=3791.54) τ_3 = 9.43 (B_3=3343.65)	4.56 26.68 68.76
GB-CDs + Fe^{3+}	5.69	1.120	τ_1 = 0.79 (B_1=3213.63) τ_2 = 3.45 (B_2=4342.62) τ_3 = 7.95 (B_3=2487.93)	6.08 40.48 53.44

The fluorescent decay profile of GB-CDs was fitted by a tri-exponential function. Chi-square values and corresponding residual distribution were reduced to judge the best fit. The acceptable fit has a chi-square close to unity.

The fitting system of the fluorescence emission intensity decay $I_{(t)}$ uses a tri-exponential representation according to the equation 4.2.

$$I_{(t)} = B_1 \exp(- t / \tau_1) + B_2 \exp(-t / \tau_2) + B_3 \exp(-t / \tau_3) \quad \textbf{4.2}$$

Where τ_1 , τ_2 and τ_3 represents time constants of the three radiative decays channel and B_1, B_2, B_3 are three corresponding amplitudes.

The following equation 4.3 was used to calculate the average life time-

$$< \tau > = \frac{B_1 \tau_1^2 + B_2 \tau_2^2 + B_3 \tau_3^2}{B_1 \tau_1 + B_2 \tau_2 + B_3 \tau_3} \quad \textbf{4.3}$$

This fluorescence quenching was proved by a photograph taken in UV-light (λ_{ex}= 365 nm) (inset **figure 4.10A**). Moreover, the quenching constant was calculated by standard Stern-Volmer **Equation 4.4** which also determines the binding attraction between the fluorescent molecule and quencher molecule.

$$F_0 / F = 1 + k_{sv}.[Q] \qquad \textbf{4.4}$$

Where F_0 is the fluorescent intensity of GB-CDs, F is the fluorescent intensity of GB-CDs in the presence of quencher (Fe^{3+}), Q is the concentration of quencher, and k_{sv} represent quenching constant. The k_{sv} value of as- prepared GB-CDs was calculated to be 0.385 $(\mu M)^{-1}$ with a correlation coefficient (R^2) of 0.9808. Moreover, the Stern-Volmer plot showed a good linear range over the concentration of Fe^{3+}, ranging from 2 to 6 µM (**Figure 4.10B**). The LOD was measured to be 0.62 µM having signal to noise ratio (S/N) of 3, while according to the U.S. environmental protection agency, the detection limit of Fe^{3+} ion in drinking water is ~5.357 µM [Shangguan *et.al*. (2017)], and also the calculated LOD was lower than those of earlier reported carbon-based nanomaterials **(Table4.3)** [Ananthanarayanan *et.al*. (2014), Yu *et.al*. (2016), Wang *et.al*. (2012), Zhang *et.al*. (2013), Li *et.al*. (2016), Liu *et.al*. (2015), Hamishehkar *et.al*. (2015), Fong *et.al*. (2015), Lu *et.al*. (2015)]. In addition, we also compared the analytical performance of as-synthesized GB-CDs with other carbon dots, derived from natural resources (**Table 4.4**) [Atchudan *et.al*. (2017), Aslandas *et.al*. (2015), Edison *et.al*. (2016) Atchudan *et.al*. (2018)] [Atchudan *et.al*. (2018)]. Therefore, the proposed CDs could be promising nanoprobe for the detection of Fe^{3+} ion.

Table 4.3 Comparison of Sensing performance of as-prepared GB-CDs with other carbon-based nanoprobes.

Detection probe (CDs)	Detection limit (μM)	Linear range (μM)	Quantum yield (%)	Reference
GQDs	7.22	0-80	10	46
NCQDs	4.67	0-50	17.8	47
GO-nanosheets	17.5	14.3-143.2	0.7	48
Graphite electrode	1.8	10-200	11.2	49
N-CDs	10.8	50-300	9.4	50
N doped CDs	10.98	0-50	0.7	51
CDs	6.05	0.16-1.66	---	52
CNPs	1.06	0-25	5.42	53
N-CDs	0.80	6-200	15.13	54
GB-CDs	0.62	2- 6	38.5	**Present work**

Table 4.4 Comparison of the analytical performance of as-prepared GB-CDs with other carbon-based nanoprobes, derived from natural resources.

Detection probe (C-based)	Detection limit (μM)	Linear range (μM)	Quantum yield (%)	Reference
C. retusus fruit	70	0-2	9	55
Blueberry	9.97	12-100	-	55
P. avium fruit	0 .96	0-100	13	57
Phyllanthus acidus	0.9	2-25	14	58
Magnolia liliifrora	1.2	1-1000	11	59
A. lakoocha	0.62	2- 6	38.5	**Present work**

4.5. Investigation of Fe^{3+} in real samples

The practical water samples spiked with different concentrations of Fe^{3+} was used to determine the accuracy test. It can be seen from Supporting Information **Table 4.5** that, in spiked water samples, the detection efficiency of Fe^{3+} varied from 92.0 **%** to 94.0 %, enlightening the practical method for Fe^{3+} detection in real samples.

Table 4.5 Fe^{3+} ion detection in spiked water sample by using GB-CDs.

Added (µM)	Found (µM)	Recovery (%)
20	18.4	92.0 %
40	37.6	94 %
60	55.5	92.5%
80	74.6	93.2%

av RSD = 92.93

The practical evaluations of as-prepared GB-CDs were also approved in human serum. It can be seen a continuous decrease in the fluorescence intensity ratio (F/F_0) having a linear relation in opposition to the volume of human serum (**Figure 4.12),** revealing the capabilities of GB-CDs for the determination of the unknown concentration of Fe^{3+} in commercial human blood serum.

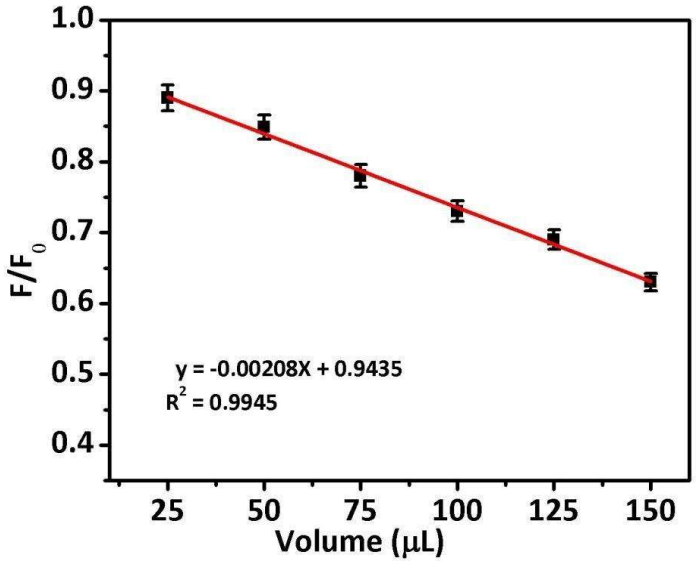

Figure 4.12 showing the correlation amid fluorescence intensity ratio (F/F0) of GB-CDs anddifferent volume of human serum added.

4.6. Detection of Fe^{3+} in the living cell

In order to intracellular sensing of Fe^{3+}, cytotoxicity assay was performed on SH-SY5Y neuroblastoma cells. **Figure 4.13(A)** shows that about 80% of cells were viable after incubation of SH-SY5Y neuroblastoma cells with GB-CDs over a wide concentration range from 0.01-200 µg/mL for 24 hours. Addition to this, there was no significant change observed in the cell viability after incubation of 48h (**Figure 4.13B**). This observation revealed that as-prepared GB-CDs have a low toxic effect on these cells, demonstrating the capability to serve as an efficient nanoprobe for the detection of fe^{3+} in living cells.

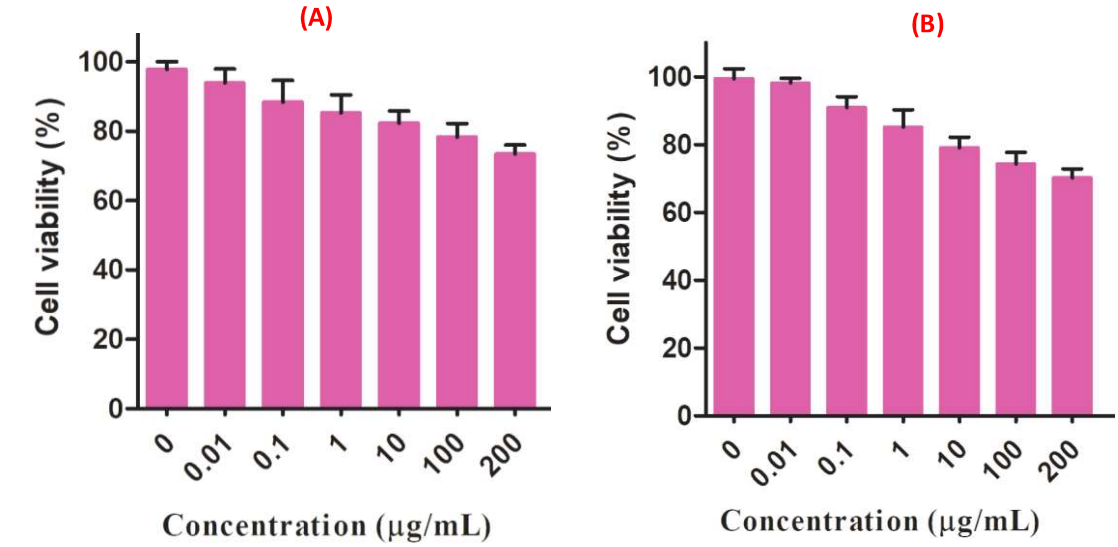

Figure 4.13 Cell viability assays of GB-CDs on SH-SY5Y neuroblastoma cells after incubation of 24h (A) and 48h (B).

Subsequently, the biosensing performances of GB-CDs in the living cells were also carried out. As shown in **Figure 4.14,** GB-CDs incubated with SH-SY5Y neuroblastoma cells displayed green and red fluorescence to the laser excitation at 485 nm and 560 nm respectively, revealing the capabilities of GB-CDs to pierce into the cell membrane. However, after incubation of 100 µL Fe^{3+} ion (10^{-3} M) into SH-SY5Y neuroblastoma cells, the fluorescence emission was finally quenched, proving the abilities of GB-CDs for the intracellular sensing of Fe^{3+} ion.

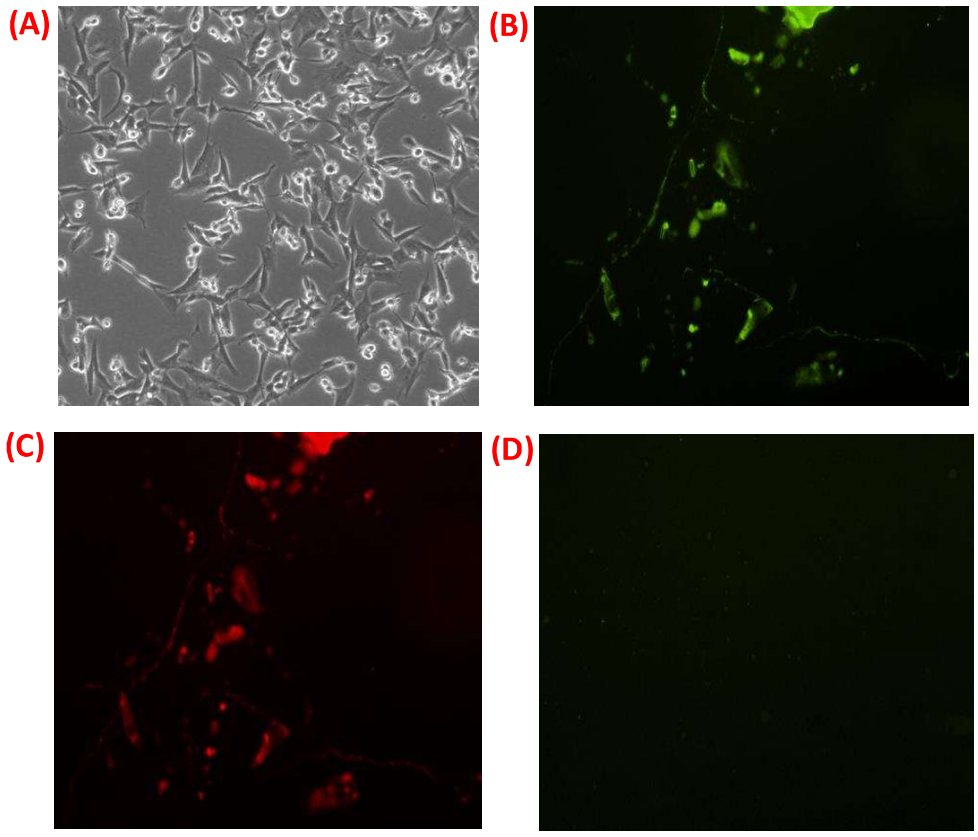

Figure 4.14 (A) Inverted light microscopy image of SH-SY5Y neuroblastoma cells without GB-CDs, (B) Fluorescent microscopic image of GB-CDs at 485nm excitation, (C) Fluorescent microscopy image of GB-CDs at 560 nm excitation, (D) Fluorescence quenching of GB-CDs after addition 100 µL of Fe^{3+}.

The practical evaluations of as-prepared GB-CDs were also approved in human serum. It can be seen a continuous decrease in the fluorescence intensity ratio (F/F_0) having a linear relation in opposition to the volume of human serum (**Figure 4.15),** revealing the capabilities of GB-CDs for the determination of the unknown concentration of Fe^{3+} in commercial human blood serum.

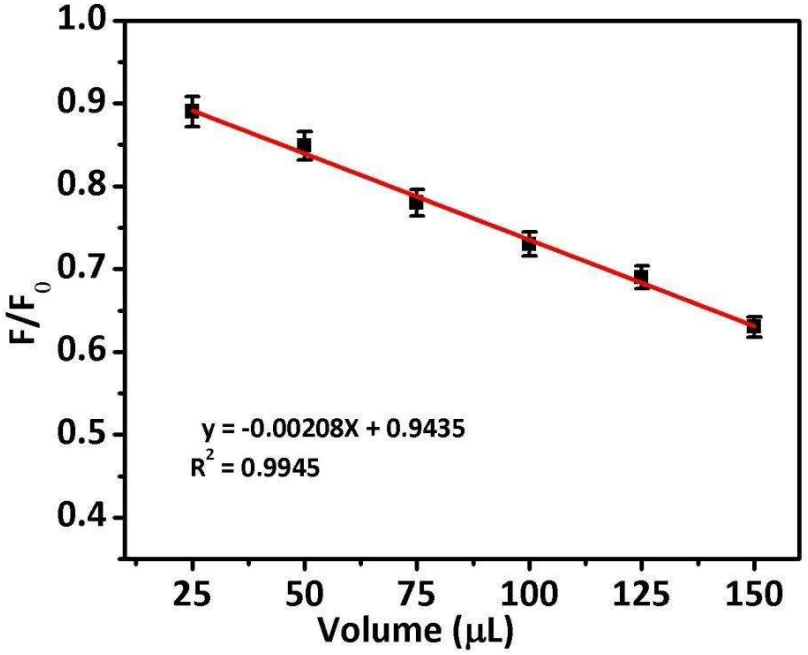

Figure 4.15 showing the correlation amid fluorescence intensity ratio (F/F0) of GB-CDs and different volume of human serum added.

4.7. Conclusions

A facile one-pot hydrothermal method has been adopted to synthesize GB-CDs from *Artocarpus lakoocha* seeds without the passivation of any chemical materials. The as-prepared GB-CDs exhibited an excitation-dependent fluorescent emission spectrum and high photostability. Outstandingly, GB-CDs were applied for the selective and sensitive detection of Fe^{3+} with an appreciable fluorescent QY of about 38.5 % using quinine sulfate as a reference. The LOD was

calculated to be 0.62 μM with linearity from 2 to 6 μM. Further, the sensing system was applied in water sample as well as in human blood serum which shows their practical applications. In addition, MTT assay was performed on SH-SY5Y neuroblastoma cells and results revealed that highly water-soluble GB-CDs have high cell viability up to 80% and have negligible cytotoxicity. Therefore, it could be utilized as a promising fluorescent nanoprobe for the diagnosis of Fe^{3+} related disease.